https://doi.org/10.3311/PPme.23845

Periodica Polytechnica Mechanical Engineering, 68(3), pp. 187–195, 2024

Oscillatory Potential-based Characterization of the Human Light-adapted Electroretinogram Using Discrete Wavelet Transform

Min Gao[1], Mirella Telles Salgueiro Barboni[2], Viktória Szabó[2], Zoltán Zsolt Nagy[2], Ditta Zobor[2], Balázs Vince Nagy[1*]

[1] Department of Mechatronics, Optics and Mechanical Engineering Informatics, Facalty of Machanical Engineering, Budapest University of Technology and Economics, Műegyetem rkp. 3, H-1111 Budapest, Hungary
[2] Department of Ophthalmology, Facalty of Health science, Semmelweis University, Vas utca 17, H-1088 Budapest, Hungary
[*] Corresponding author, e-mail: nagyb@mogi.bme.hu

Received: 13 November 2023, Accepted: 08 July 2024, Published online: 13 July 2024

Abstract

Purpose: Our aim was to apply multiple discrete wavelet transformation (DWT) types to healthy light-adapted (cone) electroretinogram (ERG) signals in order to optimize DWT analysy in ERG. Oscillatory potentials (OP) were individually extracted from the signals and used to calculate an indicator for ERG analysis.

Methods: Light-adapted (LA) 3.0 cd.s/m^2 ISCEV standard ERGs were recorded from both eyes of 15 healthy volunteers (mean age: 36.9 ± 13.0 years old; 13 females). LA ERG signal components, such as b-wave and OPs, were analyzed using the discrete wavelet transformation (DWT). An index (%OPi) was proposed to estimate the individual oscillatory potentials (OP1-OP5) by calculating the coefficient ratio of the OP to b-wave. Multiple mother wavelet functions (i.e., Daubechies, Symlet, and Coiflet) with five orders were applied and compared statistically using Wilcoxon tests and paired t-test comparisons with Bonferroni posthoc analyses ($p < 0.005$).

Results: OP4 shows the most energy at both low and high-frequency bands (80Hz and 160Hz), while OP2 has lower energy at the low-frequency band (80Hz) and higher energy at the high-frequency band (160Hz). The %OP2 is the largest among the five individual OPs. %OPs obtained with different wavelet functions differ from each other. Db2 and sym2 seem to be the optimal wavelets for analyzing light-adapted ERG components.

Conclusion: Individual OPs of the light-adapted ERG obtained with the DWT analysis may characterize different levels of retinal dysfunction. The %OPi may serve as an indicator in ERG analysis.

Keywords

electroretinogram, oscillatory potentials, discrete wavelet transformation, mother wavelet function

1 Introduction

Electroretinography (ERG) is a widely used clinical and research technique to characterize retinal functions and corresponding diseases [1, 2]. The clinical ERG signal is a summed light-evoked response of activated retinal cells, and it is comprised with few components, such as a-wave, b-wave, oscillatory potentials (OPs), i-wave, and PhNR, according to the ISCEV (International Society for Clinical Electrophysiology of Vision) standards [3]. Oscillatory potentials (OPs) , which are five small peaks (OP1 – OP5) on the rise of the b-wave, may reflect the inner retinal layers [4–6] and the specific layer is still under study. Generally, the OPs is hardly detected and measured in the full signal waveform using time domain analysis. Therefore, the ISCEV standard describe the frequency analysis method for the OPs under dark-adapted condition [3], however, there is no any method for the light-adapted (LA) OPs.

We have recently applied Fast Fourier Transform (FFT) with low cutoff frequencies (60Hz – 100Hz) to filter and analyze individual OPs, primarily OP2, OP3, and OP4, of the dark- and light-adapted healthy human full-field ERGs [7]. In that study we demonstrated a significant impact of the cutoff frequency of the digital filter on the amplitudes of the light-adapted OPs but no significant effect on the peak times. Moreover, the FFT spectrum contains a frequency range in which b-wave and OPs may overlap and are indistinguishable without temporal information.

Cite this article as: Gao, M., Barboni, M. T. S., Szabó, V., Nagy, Z. Z., Zobor, D., Nagy, B. V. "Oscillatory Potential-based Characterization of the Human Light-adapted Electroretinogram Using Discrete Wavelet Transform", Periodica Polytechnica Mechanical Engineering, 68(3), pp. 187–195, 2024.
https://doi.org/10.3311/PPme.23845

The clinical implication is that light-adapted b-wave may be affected by OP alterations and vice-versa. Nevertheless, the data showed that it is difficult to isolate OPs from the light-adapted ERG using FFT. Hence, signal analysis, such as wavelet transformation, considering both the time and the frequency information (continuous wavelet transformation (CWT) / discrete wavelet transformation (DWT)) may be clinically relevant to evaluate light-adapted ERG signals. These methods are widely used to analyze non-stationary and time-limited signals [8], such as EEG [9–11], ECG [12, 13], and also applied in ERG analysis [14, 15].

In the past 20 years, a few studies reported the benefits of DWT [16–19] and the CWT [20–24] to analyze ERG signals. Varadharajan et al. [16] in 2000 first applied the time-frequency domain analysis to differentiate ERG signals of Duchenne muscular dystrophy patients from control ERGs at two different frequency bands. More recently, Barraco et al. [20, 25] applied the CWT to analyze the ERG a-wave from controls and patients with achromatopsia. Dimopoulos et al. [26] investigated the effects of aging on inner retinal function by analyzing ERGs with CWT. The authors found that the amplitudes of the light-adapted OPs at high frequency (>120 Hz) were age-independent between 20 and 60 years or more. Gauvin et al. assessed the contribution of the OPs to the LA ERGs using DWT and considered OPs as a unique component when analyzing them [27]. To the best of our knowledge, there is no report concerning individual OPs (five peaks) contributing to the light-adapted ERG using time-frequency domain analysis. The purpose of the present study was to analyze individual light-adapted ERG OPs in the time-frequency domain using DWT in controls. In addition, the effects of the mother wavelet functions on the evaluation of individual OPs were investigated in order to find the most efficient wavelet type for ERG analysis.

2 Methods

2.1 Participants and ERG examination

Participants were 15 healthy volunteers with mean age = 36.9 ± 13.0 years old (13 females). The ERG signals were recorded from both eyes simultaneously using the RETiport system (Roland Consult, Brandenburg, Germany) equipped with the Q450 SC Ganzfeld stimulator. Pupils were dilated with tropicamide 1%, an active ERG jet electrode was placed on the corneal surface, and ground and reference skin electrodes were placed on the external canthi and forehead. The complete ISCEV standard full-field ERG protocol was applied [3]. However, only the light-adapted flash responses were analyzed in this study. Light-adapted flash intensity was 3.0 cd.s/m^2 delivered on a 30 cd/m^2 rod-saturating background after 10 minutes of light adaptation. ERG signals were 512 points in 150 ms, including a 16 ms pre-stimulus period. The experiment was performed in accordance with the declaration of Helsinki and approved by the institutional ethics committee. All participants signed consent before the tests after explaining the nature and possible consequences of the study.

2.2 Discrete wavelet analysis

The limitation of the Fourier transformation analysis is that the spectrum contains only frequency information after transforming the signal, but the electrophysiological signals are transitory, and their frequency contents change over time. Hence, temporal information is as important as frequency when analyzing it. The wavelet transform is an advanced signal analysis method in non-stationary signals, such as electrophysiological signals, displaying time-frequency representation. The wavelet transform decomposes signals into a set of basis functions by scaling(compressing or stretching) and shifting a mother wavelet (i.e., window function), which is a finite-length, oscillating, zero-mean waveform [28]. Analysis of a time series by DWT requires a set of functions obtained from the mother wavelet ($\varphi(t)$), which is expressed as:

$$\varphi_{j,k}(t) = 2^{-\frac{j}{2}}\varphi\left(2^{-\frac{j}{2}}t - k\right) \tag{1}$$

Where j is scale parameter, which is related to the frequency band and adapts the width of the mother wavelet (φ) to the required resolution; and k is shift parameters, which is related to the temporal position of the window and used to localize the analyzed signal. $2^{j/2}$ is the normalization factor that ensures the same energy for the whole "j" and "k" [24]. When a mother wavelet is given, DWT of a signal $x(t)$ is expressed by the convolution of $x(t)$ with the complex conjugate of $\varphi(t)$, given by the Eq. (2):

$$C(j,k) \le x(t), \varphi_{j,k}(t) \ge \frac{1}{\sqrt{2^j}} \int_{-\infty}^{\infty} \varphi \cdot \left(\frac{t - 2^j}{k \cdot 2^j}\right) x(t)\, dt \tag{2}$$

Where C is the transform coefficient, functioning with the scale j (deciding the oscillatory frequency and the length of the wavelet) and shift factor k (determining its shifting position). In Eq. (2), the main factor is the mother wavelet which contains several characters [28] (i.e., orthogonality, compact support, symmetry, and vanishing moment).

Different types of mother wavelets may result differently when applied to the same signal, because when appling the wavelet transformation, small windows capture low frequency resolution content and provide good temporal localization, while large windows capture low temporal resolution along with good frequency resolution. Therefore, the selection of a suitable mother wavelet is crucial. In this study, we selected the simplest mother wavelet, which is Haar wavelet, and three orthogonal mother wavelet types, such as Daubechies, Symlets, and Coiflet, to analyze light-adapted ERGs and to recommend references for the selection of the mother wavelet.

The DWTs of ERG signals were performed with a self-developed code in Matlab (Mathworks, Natick, MA, USA), and the DWT scalograms to display the time-frequency information were plotted using the absolute coefficient values. Before DWT computation, each response was padded to 1024 points by repeating the first and last values on both sides of the signal to reduce edge effects [29].

2.3 Individual oscillatory potentials

Mean control ERG signal (Fig. 1(a), blue plot) with filtered OPs (Fig. 1(a), orange plot) and corresponding DWT scalogram (Fig. 1(b)) with eight levels (i.e., eight frequency bands) are shown in Fig. 1 to explain individual oscillatory potentials (OPs) definition in the time-frequency domain. The OPs were filtered with the cutoff frequency of 160Hz – 300Hz (orange plot in Fig. 1(a)) and showed five main peaks (i.e., OP1 – OP5) in the time domain. In the frequency domain the ERG b-wave is low frequency dominated while OPs are found primarily at higher frequency. According to the previous work of Gauvin [30], two low-frequency bands centered at 20 Hz (L-b) and 40 Hz (H-b) representing the b-wave and two high-frequency bands centered at 80 Hz (L-OPs) and 160 Hz (H-OPs) representing the OPs were quantified in the DWT scalogram. According to the wavelet transformation theory, each frequency band's time resolution is different, and it's higher at high frequency bands and lower at low-frequency bands.

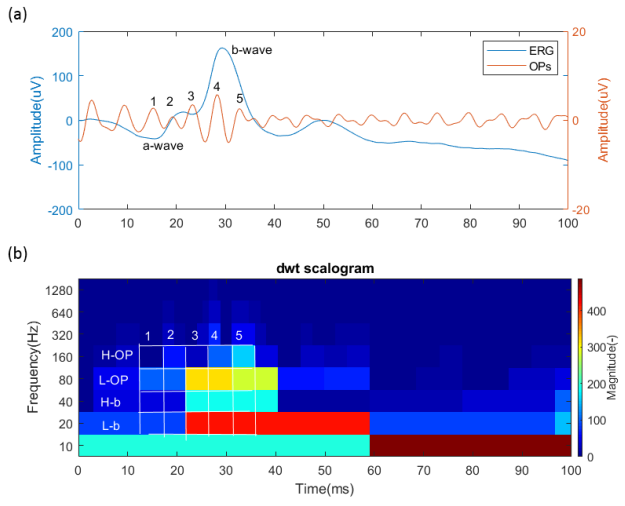

Fig. 1 Mean control ERG signal and filtered OPs in the time domain are shown in (a). The DWT scalogram is shown in (b), which displays the central frequency of each band (y-axis), time information (x-axis) same as the signal time, and the coefficient magnitude (right scale) of each time-frequency bin (maximal values are shown in red and minimum values are shown in blue). *B*-wave and OPs are represented in two horizontal frequency bands (*L-b* and H-b) and (*L-OP* and *H-OP*), respectively, and five individual OPs are indicated in the columns 1–5.

Moreover, our previous work [7] showed that the control OP4 coincides with the b-wave in time, and the peak times of other individual OPs were relatively constant when the cutoff frequency increased. The temporal resolution at 160 Hz band coincides with the peak time of OPs (OP1 – OP5) as shown in Fig. 1(a) and Fig. 1(b). These five individual OPs are indicated by the columns (1–5) in Fig. 1(b). Four frequency bands of interest representing the b-wave and OPs are divided into 20 time-frequency bins, DWT coefficients of each bin shown in scale (maximal values are shown in red and minimum values are shown in blue). The coefficient ratio of the individual OP to the *b*-wave was calculated based on the Eq. (3)

$$\%OP_i = \frac{H\text{-}OP_i + L\text{-}OP_i}{H\text{-}OP_i + H\text{-}OP_i + H\text{-}b_i + L\text{-}b_i} \cdot 100\% \tag{3}$$

Where i is the OP in the i^{th} range, *H-OP*, *L-OP*, *H-b*, and *L-b* are the DWT coefficients in each corresponding bin.

2.4 Mother wavelet selection

The criteria for selecting the optimal wavelet in this study was performed by claculating the ratio of energy to Shannon entropy [31, 32] as shown in Eq. (4).

$$\text{ratio} = \frac{\text{Energy}}{\text{Shannon entropy}} \tag{4}$$

where the energy was the sum of all the wavelet coefficients squared of the selected bins for each wavelet. Shannon entropy was calculated by the plug-in estimator [33], which is a technique to estimate the entropy, for all the coefficients over 20 bins as shown in Eq. (5).

$$H = -\sum_k p_k \ln\left(p_k\right), \tag{5}$$

where H is the Shannon entropy for the k bins, and p_k is the possibility of the k^{th} bins calculated by dividing the coefficient of k^{th} bin by the summed coefficients of all bins (20 bins). The lower Shannon entropy indicates the less uncertainty and higher energy indicates more suitable for the transformation. Hence, the higher ratio indicates the better wavelets.

2.5 Statistical analysis

Data are expressed as mean ± standard deviation of the mean. The effects of mother wavelet function on %OPs were evaluated using Wilcoxon tests and paired t-test comparisons with Bonferroni post-hoc analyses (SPSS, Statistical Package for the Social Sciences, Hong Kong, China), multiple comparisons corrected p values <0.0005 were considered statistically significant.

3 Results

3.1 Individual oscillatory potential analysis with Haar wavelet function

Fig. 2 shows the analysis of the control ERG using Haar wavelet as the mother wavelet function when applying the discrete wavelet transformation (DWT). Four representative subject signals (Fig. 2(a)) selected from the individual control ERG signals (Fig. 2(b)) of the mean b-wave amplitude of 214 ± 44.6 uV and peak time of 29.6 ± 1.2 ms are shown. The corresponding scalograms are shown under the signal. The coefficients of each bin are shown in the colormap, where the maximal values are limited to 500 (colored in red) for the purpose of comparison. The white rectangles indicate the region of interest (i.e., H/L-OP/b frequency bands in 1–5 intervals).

Fig. 2(c) illustrates DWT's mean individual oscillatory potential (OP) analysis. B-wave and OPs both have higher coefficients in low-frequency bands (L-b and L-OP) shown in gray and light blue columns, respectively, while OP2 and OP4 have higher coefficients in the high-frequency band (H-OP), and OP4 is the biggest one (110.4 ± 41.3). %OP (mean ± standard deviation) calculated with the proposed method are shown in red square and line (right y-axis). %OP1 (41.7% ± 11.7%) and %OP2 (55.9% ± 16.8%) are higher than the others (%OP3 – %OP5). %OP2 is significantly higher than others ($p < 0.0005$), while %OP3 (35.9% ± 5.9%) is significantly lower than others ($P < 0.0005$). %OP4 is not significant different with %OP1 and %OP5 ($P = 0.17$ and $P = 0.56$).

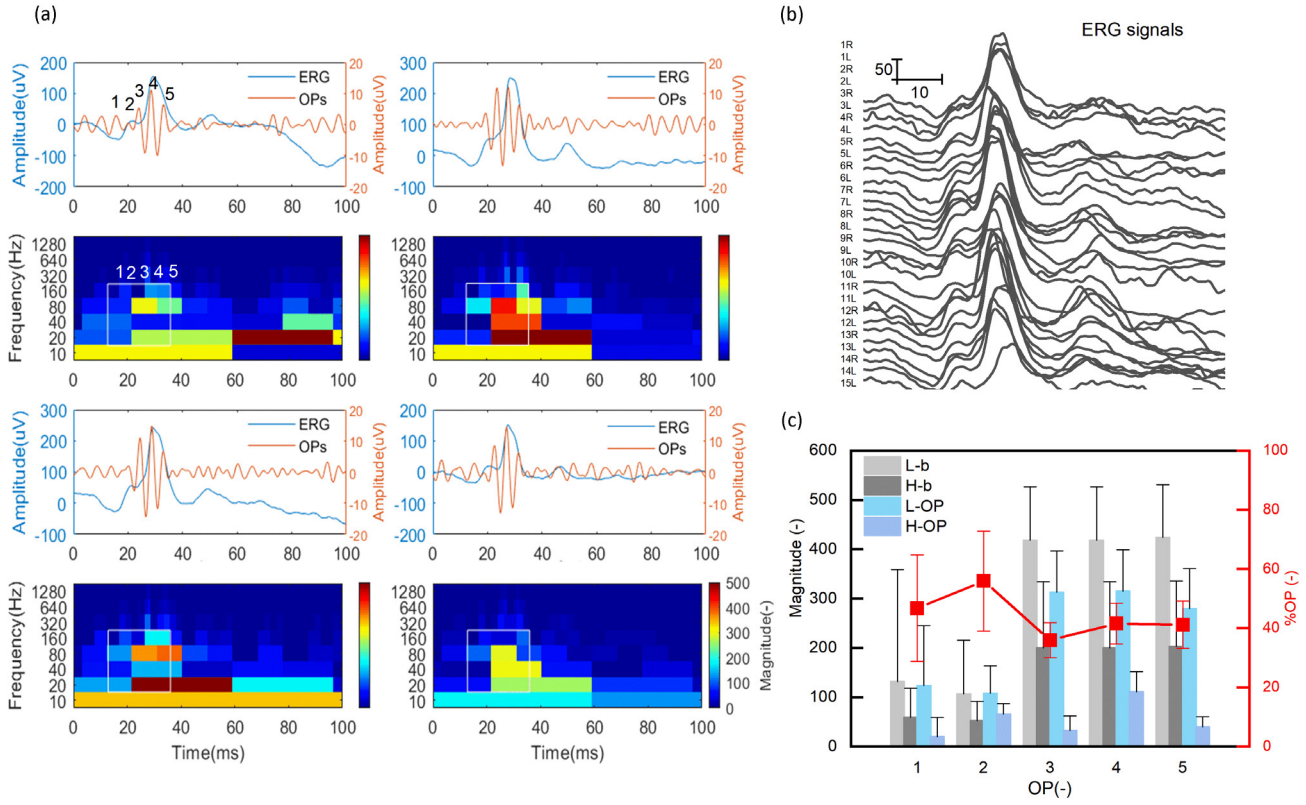

Fig. 2 The DWT analysis with Haar wavelet function. Four representive control ERG signals (blue line) and filtered OPs (orange line) in time domain and corresponding scalogram (in colored map) underneath in time-frequency domain (a) selected from the individual subjects (b) are shown. The DWT coefficient magnitude (colored columns) analysis of each selected bin and the calculated %OP (red square and line) are shown in (c).

3.2 Impact of the mother wavelet functions on the oscillatory potentials' ratios (%OP)

Three orthogonal mother wavelet families (i.e., Daubechies (db), Symlet (sym), and Coiflet (coif)) with five orders of N = 2, 4, 6, 8, 10 (shown in Fig. 3(a)) were utilized to analyze the individual OP of normal subjectsusing our proposed method. In Fig. 3(a), each row indicates one wavelet family, where Daubechies (db) show more assymmetry while Symlet (sym) and Coiflet (coif) are closely symmetric. Each column indicates one order ,where the N of dbN and symN stands forthe order , while the order is 2N of coifN for each wavelet. Fig. 3(b) shows the scalograms obtained from the mean control ERG signal with the abovementioned mother wavelets and scaled to the same maximum coefficient magnitude (red in 500) for comparison. The white squares highlight the region of interest in each scalogram.

The results gained with the different wavelet functions differ from each other. The relationships between %OPs and mother wavelet order (db : blue; sym : orange; coif : green, and haar : black dotted line) are shown in Fig. 3(c) and indicate that the %OP1 and %OP2 have similar patterns while %OP3, %OP4, and %OP5 show a mirrored pattern to the previous two. The %OPs obtained with different orders of Daubechies (db) are oscillating while that of Symlet (sym) and Coiflet (coif) change evenly with order (the %OP1 and %OP2 decrease while %OP3-%OP5 increase with increasing the order of both sym and coif wavelets). %OP1, %OP2 and %OP5 obtained from sym and coif don't show any significant difference ($p > 0.005$) at each order except for the 2nd order while that of db shows a significant difference ($p < 0.005$) from sym and coif except for the 8th order, at which the individual %OPs reach similar values ($p > 0.005$) for all three wavelets.

The ratios for optimal wavelet selection of energy to Shannon entropy are shown in Fig. 4 where the higher value indicate the better discrete wavelets. The Symlet wavelet family is relatively stable throughout all orders expect for the 2nd order while the Coiflet wavelet family

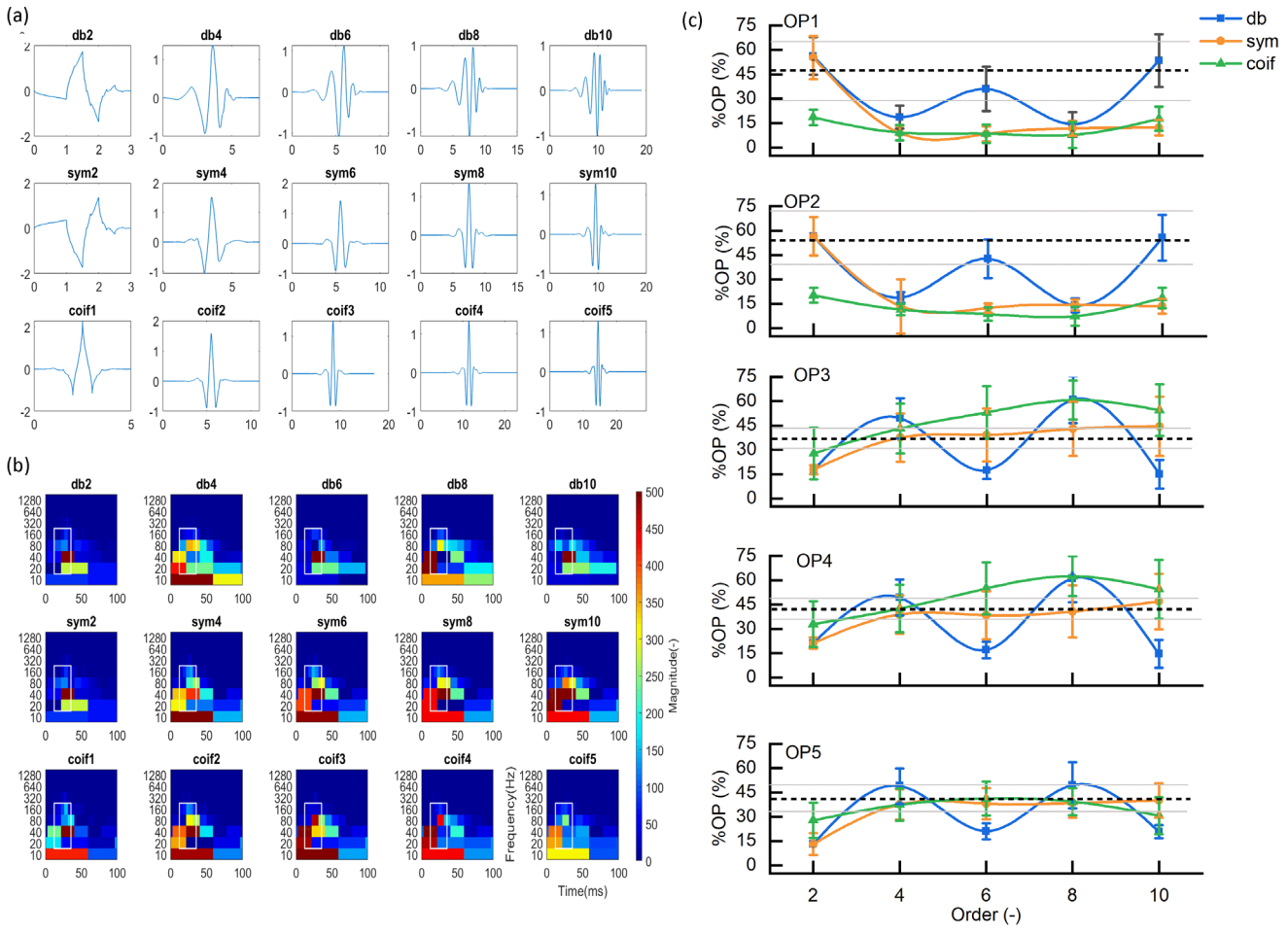

Fig. 3 Multiple analyses using three mother wavelet families. (a) shows the waveforms of three mother wavelets, rows indicate wavelet name family, and columns indicate the orders of the wavelets. The corresponding DWT scalograms of the mean ERG signal are shown in (b). The correlation between %OPs and wavelet orders are shown in (c), and the black dotted lines and gray lines indicate the mean and standard deviation values obtained from the Haar wavelet.

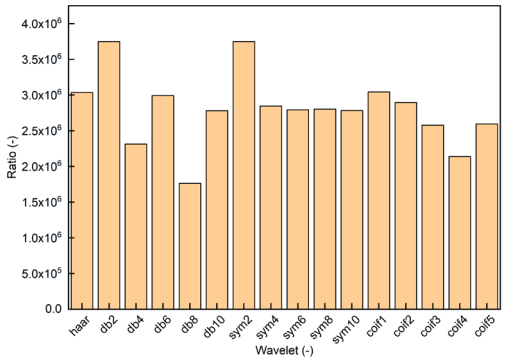

Fig. 4 Energy-to-entropy ratio obtained with all wavelets. Higher values indicate better discrete wavelets for the decomposition.

results decrease with increasing the wavelet order from 2nd to 8th. The Daubechies show unstable ratio values when the order changes. Based on this evaluation db2 and sym2 seem to be the most suitable wavelets for evaluating %OPs among all the wavelets, while db8 gives lowest results.

4 Discussion

The purpose of this work was to study the human light-adapted electroretinogram (LA ERG) fast component, the oscillatory potential (OP), in the time-frequency domain using discrete wavelet transform (DWT), and to study how the mother wavelet characteristics affect the OP analysis. This study investigated an approach to analyze the individual OP (i.e., OP1 – OP5) by separating the DWT coefficient in five time windows (1–5) and four frequency bands (H/L-OP, H/L-b) and by the term of ratio %OPi, the coefficient ratio of OP to b-wave in each time bin. The results show that the individual OPs contributed differently to the b-wave and the mother wavelet function affected the results differently.

This study is a continuation of our previous work [7] analyzing the OPs using FFT, adding time domain investigation. Here we applied the discrete wavelet function to transform the ERG signal from the time domain to the time-frequency domain and defined four frequency bands in the frequency axis for both b-wave and OPs, which is consistent with Gauvin's work [23]. Moreover, in the time axis, we specified five time intervals according to both the theory of wavelet transform [28] and our previous study [7]. The peak times of the individual OPs matches the time resolution at the higher frequency band (160 Hz), as shown in Fig. 1. This made it more precise for analyzing the OPs than Gauvins' work since their OPs peak time exceeded b-wave (i.e., 17.5 – 55 ms, while the b-wave peak time is at: 30.98 ± 1.33 ms). We also calculated the %OP by calculating the ratio of summed OP coefficients to b-wave and obtained that the sum %OP is 41.2% ± 5.8%, which is lower than their result (56.6% ± 2.5%), using the same Haar mother wavelet. This is because ERG signals are somewhat different due to the different recording systems. Our ERG signal didn't show obvious OP3, while there was obvious OP3 in their signal. In our finding OP3 contributes the least to the b-wave. The summed %OP (41.2% ± 5.8%) contributes less than half to build the b-wave, which is consistent with the previous studies using band-pass filter to extract the Ops [34–36].

We found that OP2 and OP4 have higher energy than other OPs at 160 Hz (H-OP) band, and OP4 has much higher energy than OP2 at 80 Hz (L-OP) band. However, the %OP2 (55.9% ± 16.8%) was the biggest among five %OPs, while %OP4 was 41.6% ± 6.8%. which means the OP2 contributes the most to the b-wave. It is an interest founding since that the OP4 was thought to contribute the most to the b-wave due to the coincidence of the b-wave in peak time. the %OP3 (35.9% ± 5.9%) was the lowest among the five OPs indicating that the OP3 contributes the least to the b-wave, which was consistent with the ERG signal. Our finding of the different %OP may confirm the different inner cells of the retina generating individual Ops [37] since pharmacological interventions blocking the activation of specific cells affect the OPs differently [38]. Moreover, different retinal origins of the OPs are also supported by previous findings in congenital stationary night blindness (CSNB) that LA OP2 and OP3 are absent while OP4 is spared [39]. The origin of individual OPs might emphasize the clinical value, in addition to main ERG components.

Comparing mother wavelet types Symlet (sym) and Coiflet (coif) wavelets had similar effects on the analysis of individual OPs while Daubechies (db) wavelet had a different effect. This may be caused by the symmetry characters, where Daubechies has less symmetry than Symlet and Coiflet. Our examination showed the db2 and sym2 to be the most indicative wavelets for analyzing human ERG signals according to the energy-to-Shannon entropy ratio. It may be because db2 and sym2 wavelets have two zero-mean waveforms that match well with the ERG signal itself. They both showed a higher %OP1 and %OP2 than %OP3-%OP5. Db8 is not suggested for analyzing the ERG signal since the ratio is the lowest. All Symlet wavelets are recommended since they do not change much with the different orders.

Further investigations of LA ERG fast component %OPs should be applied to evaluate patients groups, such as diabetic retinopathy (DR), central retinal vein occlusion(CRVO), and retinitis pigmentosa (RP) using discrete wavelets transformation with different wavelet types and orders.

5 Conclusion

Individual OPs of the light-adapted ERG obtained with the discrete wavelet transformation analysis may characterize different levels of retinal dysfunction. The ratio of OP to b-wave, which is %OP, may be an indicative parameter of ERG results.

Funding

The research reported in this paper is part of project no. BME-NVA-02, implemented with the support provided by the Ministry of Innovation and Technology of Hungary from the National Research, Development, and Innovation Fund, financed under the TKP2021 funding scheme. This research was funded by the National Research, Development, and Innovation Fund of Hungary under Grant TKP2021-EGA-02. The research was supported by Stipendium Hungaricum Scholarship of Tempus Public Foundation, and China Scholarship Council (202002890007) to GM. Research supported by National Research, Development, and Innovation Fund of Hungary to MTSB (OTKA-PD grant number 134799) and the Tempus Public Foundation (Hungary) to MTSB (TKA grant number 167949).

Conflict of interest

All authors certify that they have no affiliations with or involvement in any organization or entity with any financial interest (such as honoraria; educational grants; participation in speakers' bureaus; membership, employment, consultancies, stock ownership, or other equity interest; and expert testimony or patent-licensing arrangements), or non-financial interest (such as personal or professional relationships, affiliations, knowledge or beliefs) in the subject matter or materials discussed in this manuscript.

Ethical approval

All procedures performed in studies involving human participants were in accordance with the ethical standards of the Institutional ethics committee of the Semmelweis University and with the 1964 Helsinki declaration and its later amendments or comparable ethical standards. Informed consent was obtained from all individual participants included in the study.

References

[1] Moschos, M. M., Gouliopoulos, N. S., Kalogeropoulos, C. "Electrophysiological examination in uveitis: A review of the literature", Clinical Ophthalmology, 8, pp. 199–214, 2014. https://doi.org/10.2147/OPTH.S54838

[2] Young, B., Eggenberger, E., Kaufman, D. "Current electrophysiology in ophthalmology: A review", Current Opinion in Ophthalmology, 23(6), pp. 497–505, 2012. https://doi.org/10.1097/ICU.0b013e328359045e

[3] Robson, A. G., Frishman, L. J., Grigg, J., Hamilton, R., Jeffrey, B. G., Kondo, M., … McCulloch, D. L. "ISCEV Standard for full-field clinical electroretinography (2022 update)", Documenta Ophthalmologica, 144, pp. 165–177, 2022. https://doi.org/10.1007/s10633-022-09872-0

[4] Wachtmeister, L. "Oscillatory Potentials in the Retina: what do they Reveal", Progress in Retinal and Eye Research, 17(4), pp. 485–521, 1998.

[5] Wachtmeister, L. "On The Oscillatory Potentials Of The Human Electroretinogram In Light And Dark Adaptation: IV. Effect of adaptation to short flashes of light. Time interval and intensity of conditioning flashes", Acta Ophthalmologica, 51(2), pp. 250–269, 1973. https://doi.org/10.1111/j.1755-3768.1973.tb03802.x

[6] Wachtmeister, L. "On the oscillatory potentials of the human electroretinogram in light and dark adaptation: III. Thresholds and relation to stimulus intensity on adaptation to background light", Acta Ophthalmologica, 51(1), pp. 95–113, 1973. https://doi.org/10.1111/j.1755-3768.1973.tb08251.x

[7] Gao, M., Telles, M., Barboni, S., Fix, D., Nagy, B. V. "Effects of fixed cutoff filtering on dark- and light-adapted ERG components and the application of variable cutoff filter", Documenta Ophthalmologica, 144, pp. 191–202, 2022. https://doi.org/10.1007/s10633-021-09853-9

[8] Behbahani, S., Ahmadieh, H., Rajan, S. "Feature Extraction Methods for Electroretinogram Signal Analysis: A Review", IEEE Access, 9, pp. 116879–116897, 2021. https://doi.org/10.1109/access.2021.3103848

[9] Bhati, D., Sharma, M., Bilas, R., Gadre, V. M. "Time – frequency localized three-band biorthogonal wavelet filter bank using semidefinite relaxation and nonlinear least squares with epileptic seizure EEG signal classification", Digital Signal Processing, 62, pp. 259–273, 2016. https://doi.org/10.1016/j.dsp.2016.12.004

[10] Kiymik, M. K., Güler, I., Dizibüyük, A., Akin, M. "Comparison of STFT and wavelet transform methods in determining epileptic seizure activity in EEG signals for real-time application", Computers in Biology and Medicine, 35(7), pp. 603–616, 2005. https://doi.org/10.1016/j.compbiomed.2004.05.001

[11] Al-Qazzaz, N. K., Mohd Ali, S. H. Bin, Ahmad, S. A., Islam, M. S., Escudero, J. "Selection of mother wavelet functions for multi-channel EEG signal analysis during a working memory task", Sensors, 15(11), pp. 29015–29035, 2015. https://doi.org/10.3390/s151129015

[12] Brechet, L., Lucas, M. F., Doncarli, C., Farina, D. "Compression of biomedical signals with mother wavelet optimization and best-basis wavelet packet selection", IEEE Transactions on Biomedical Engineering, 54(12), pp. 2186–2192, 2007. https://doi.org/10.1109/TBME.2007.896596

[13] Erçelebi, E. "Electrocardiogram signals de-noising using lifting-based discrete wavelet transform", Computers in Biology and Medicine, 34(6), pp. 479–493, 2004. https://doi.org/10.1016/S0010-4825(03)00090-8

[14] Barraco, R., Persano Adorno, D., Brai, M., Tranchina, L. "A comparison among different techniques for human ERG signals processing and classification", Physica Medica, 30(1), pp. 86–95, 2014. https://doi.org/10.1016/j.ejmp.2013.03.006

[15] Gauvin, M., Little, J. M., Lina, J. M., Lachapelle, P. "Functional decomposition of the human ERG based on the discrete wavelet transform", Journal of Vision, 15(16), 14, 2015. https://doi.org/10.1167/15.16.14

[16] Varadharajan, S., Lakshminarayanan, V., Gustafson, K. M. "Wavelet analysis of ERG of patients with Duchenne Muscular Dystrophy", In: Vision Science and its Application, OSA Technical Digest, pp. 65–68, 2000.

[17] Rogala, T., Brykalski, A. "Wavelet feature space in computer-aided electroretinogram evaluation", Pattern Analysis and Applications, 8(3), pp. 238–246, 2005. https://doi.org/10.1007/s10044-005-0003-9

[18] Miguel-Jiménez, J. M., Velasco, R. B., Vázquez, L. B., De La Villa Polo, P. "Multifocal electroretinography. Glaucoma diagnosis by means of the wavelet transform", In: 2008 Canadian Conference on Electrical and Computer Engineering, Niagara Falls, ON, Canada, 2008, pp. 867–870. https://doi.org/10.1109/CCECE.2008.4564659

[19] Miguel-Jiménez, J. M., Boquete, L., Ortega, S., Rodríguez-Ascariz, J. M., Blanco, R. "Glaucoma detection by wavelet-based analysis of the global flash multifocal electroretinogram", Medical Engineering and Physics, 32(6), pp. 617–622, 2010. https://doi.org/10.1016/j.medengphy.2010.02.019

[20] Barraco, R., Bellomonte, L., Brai, M. "Time-frequency behaviour of the a-wave of the human electroretinogram", IFMBE Proceedings, 16(1), pp. 919–922, 2007. https://doi.org/10.1007/978-3-540-73044-6_238

[21] Barraco, R., Persano Adorno, D., Brai, M. "An approach based on wavelet analysis for feature extraction in the a-wave of the electroretinogram", Computer Methods and Programs in Biomedicine, 104(3), pp. 316–324, 2011. https://doi.org/10.1016/J.CMPB.2011.05.001

[22] Penkala, K., Rogala, T., Brykalski, A. "Selected Methods of the Pattern Electroretinogram Signal Analysis", Pomiary Automatyka Kontrola, 53(6), pp. 22–25, 2007.

[23] Gauvin, M. "Time-Frequency Analysis of the Human Photopic Electroretinogram: Method, Normative Data and Clinical Application", PhD Thesis, McGill University, 2017.

[24] Erkaymaz, O., Senyer Yapici, Í., Uzun Arslan, R. "Effects of obesity on time-frequency components of electroretinogram signal using continuous wavelet transform", Biomedical Signal Processing and Control, 66, 102398, 2021. https://doi.org/10.1016/j.bspc.2020.102398

[25] Barraco, R., Persano Adorno, D., Brai, M. "ERG signal analysis using wavelet transform", Theory in Biosciences, 130, pp. 155–163, 2011. https://doi.org/10.1007/s12064-011-0124-1

[26] Dimopoulos, I. S., Freund, P. R., Redel, T., Dornstauder, B., Gilmour, G., Sauvé, Y. "Changes in rod and cone-driven oscillatory potentials in the aging human retina", Investigative Ophthalmology and Visual Science, 55(8), pp. 5058–5073, 2014. https://doi.org/10.1167/iovs.14-14219

[27] Gauvin, M., Dorfman, A. L., Trang, N., Gauthier, M., Little, J. M., Lina, J.-M., Lachapelle, P. "Assessing the Contribution of the Oscillatory Potentials to the Genesis of the Photopic ERG with the Discrete Wavelet Transform", BioMed Research International, 2016(1), 2790194, 2016. https://doi.org/10.1155/2016/2790194

[28] Johansson, E. "Wavelet Theory and some of its Applications", PhD Thesis, Luleå Tekniska Universitet, 2005.

[29] Torrence, C., Compo, G. P. "A Practical Guide to Wavelet Analysis", Bulletin of the American Meteorological Society, 79(1), pp. 61–78, 1998. https://doi.org/10.1175/1520-0477(1998)079<0061:APGTWA>2.0.CO;2

[30] Gauvin, M., Lina, J.-M., Lachapelle, P. "Advance in ERG Analysis: From Peak Time and Amplitude to Frequency, Power, and Energy", BioMed Research International, 2014(1), 246096, 2014. https://doi.org/10.1155/2014/246096

[31] Shigueoka, L. S., Vasconcellos, J. P. C. de, Schimiti, R. B., Reis, A. S. C., Oliveira, G. O. de, Gomi, E. S., … Costa, V. P. "Automated algorithms combining structure and function outperform general ophthalmologists in diagnosing glaucoma", PLOS ONE, 13(12), e0207784, 2018. https://doi.org/10.1371/journal.pone.0207784

[32] Sarossy, M., Crowston, J., Kumar, D., Weymouth, A., Wu, Z. "Time-Frequency Analysis of ERG With Discrete Wavelet Transform and Matching Pursuits for Glaucoma", Translational Vision Science & Technology, 11(10), 19, 2022. https://doi.org/10.1167/tvst.11.10.19

[33] Zhang, Z., Zhang, X. "A Normal Law for the Plug-in Estimator of Entropy", IEEE Transactions on Information Theory, 58(5), pp. 2745–2747, 2012. https://doi.org/10.1109/TIT.2011.2179702

[34] Kizawa, J., Machida, S., Kobayashi, T., Gotoh, Y., Kurosaka, D. "Changes of Oscillatory Potentials and Photopic Negative Response in Patients with Early Diabetic Retinopathy", Japanese Journal of Ophthalmology, 50(4), pp. 367–373. https://doi.org/10.1007/s10384-006-0326-0

[35] Lachapelle, P., Rousseau, S., Mckerral, M., Benoit, J., Polomeno, R. C., Koenekoop, R. K., Little, J. M. "Evidence supportive of a functional discrimination between photopic oscillatory potentials as revealed with cone and rod mediated retinopathies", Documenta Ophthalmologica, 95(1), pp. 35–54, 1998. https://doi.org/10.1023/A:1001784614333

[36] Holopigian, K., Seiple, W., Lorenzo, M., Carr, R. "A Comparison of Phoropic and Scotopic Electroretinogrophic Changes in Early Diabetic Refinoparhy", Investigative Ophthalmology & Visual Science, 33(10), pp. 2773–2780, 1992.

[37] Heynen, H., Wachtmeister, L., van Norren, D. "Origin of the oscillatory potentials in the primate retina", Vision Research, 25(10), pp. 1365–1373, 1985.
https://doi.org/10.1016/0042-6989(85)90214-7

[38] Wachtmeister, L., Dowling, J. E. "The oscillatory potentials of the mudpuppy retina", Investigative Ophthalmology and Visual Science, 17(12), pp. 1176–1188, 1978.

[39] Lachapelle, P., Little, J. M., Polomeno, R. C. "The photopic electroretinogram in congenital stationary night blindness with myopia", Investigative Ophthalmology and Visual Science, 24(4), pp. 442–450, 1983.